Title:

Temporal impulse response function of the visual system estimated from ocular following responses in humans

Authors:

Yusuke Ohnishi, Kenji Kawano, and Kenichiro Miura

Affiliations:

Department of Integrative Brain Science, Graduate School of Medicine, Kyoto University

Pages: 21. Figures: 3. Tables: 0.

Corresponding author:

Kenichiro Miura, PhD

Department of Integrative Brain Science

Graduate School of Medicine, Kyoto University

Konoe-cho, Yoshida, Kyoto-shi, Kyoto 606-8501, Japan

Email: kmiura@brain.med.kyoto-u.ac.jp

Phone: +81-75-753-4481

Fax: +81-75-753-4486

Abstract:

Early visual processing functions as a set of spatiotemporal image filters. Our ability to sense changes in retinal images is determined by these filters along the temporal axis. In this study, we developed a paradigm to identify the kernel of the temporal filters based on ocular following responses (OFRs) to two-frame apparent motion stimuli. We first conducted two experiments to acquire fundamental data. In the first experiment, in which a quarter wavelength step of a sinusoidal grating was presented with various inter-stimulus intervals (ISIs), we found that OFRs were reversed by the ISI, which is consistent with previous findings. In the second experiment, a quarter wavelength step of a sinusoidal grating was applied with various durations of the initial image frame (motion onset delays; MODs); we found that longer exposure to the initial image reduced OFRs. Parameters of motion energy model involving temporal filters were optimized so that the model could reproduce the dependence of OFRs on ISIs and MODs. We were then able to successfully obtain quantitative estimates of the biphasic temporal filters with optimal frequencies in 6-8 Hz. This method is completely objective and will thus be applicable to a wide range of human subjects and model animals.

Keywords

low-level vision, temporal filter, apparent motion, visual motion analysis, eye movement

Introduction

Early visual processing functions as a set of spatiotemporal image filters whose characteristics determine what/how we can see. Our ability to sense changes in retinal images is determined by filters in the temporal domain. Critical flicker (-fusion) frequency (CFF) is the highest temporal frequency of images that we can perceive changes in brightness. Thus, it is one of the measures used to describe the characteristics of the temporal filter. Contrast sensitivity (or threshold) to the flickering of images at different temporal frequencies reveals the frequency characteristics of temporal filters (Kelly, 1961a). The impulse response function of the temporal filter has been quantitatively reconstructed based on a model consisting of linear photoreactive and pulse-encoding stages (Kelly, 1961b). The temporal filter kernels have also been quantitatively estimated using double-step methods (Burr and Morrone, 1993; Hisakata and Murakami, 2008).

Two frame animations presented with inter-stimulus intervals (ISIs) induce reversed motion percepts. Shioiri and Cavanagh (1990) have suggested that this phenomenon is due to the characteristics of the temporal filters embedded in the visual system. The energy-based motion detector of Adelson and Bergen (1985) involves temporal filters with biphasic impulse response functions. This model can at least qualitatively explain the existence of illusory motion percepts in ISI experiments (Strout et al., 1994; Takeuchi and De Valois, 1997). Recently, the temporal filters have been quantitatively estimated from perceived motions using this motion energy model (Challinor and Mather, 2010). Thus, illusory motion percepts also provide clues to the nature of temporal filters. However, all of these attempts were based on subjective reports of observers.

Sudden motions of wide-field textures elicit reflexive eye movement responses. Such responses are called ocular following responses (OFRs) (Gellman et al., 1990; Miles et al.,

1986). It was suggested that low-level energy-based mechanisms of visual motion detection underlie OFRs (Miura et al., 2006; Sheliga et al., 2005). Two frame animations presented with ISIs induced OFRs in the reversed direction, as was observed with motion percepts (Nohara et al., 2015; Sheliga et al., 2006). Researchers then argued that the reversed responses are consistent with the biphasic impulse response functions of temporal filters. Since the OFRs are purely reflexive, the responses may be used as an objective measure to quantitatively identify the temporal filters in early visual processing, though there were some different response characteristics between motion perception and OFRs (Nohara et al., 2015; Sheliga et al., 2006). However, no studies have been devoted to deriving quantitative estimates of the temporal filters for the OFRs to the two-frame motion.

Here we report the development of an experimental paradigm to identify the kernel of the temporal filters based on OFRs to two-frame apparent motion stimuli. We first established a simple but novel experimental procedure to study the process of temporal filtering of images using OFRs. We then quantitatively estimated the temporal filters applied to images based on the observed data under the assumption that a motion energy model proposed by Adelson and Bergen (Adelson and Bergen, 1985) underlies the OFRs. We compared our findings to previous findings and considered our paradigm's methodological benefits and limitations.

Materials and Methods

Subjects

Eye movements were recorded from two subjects (S1 and S2, aged 29 and 44, respectively). S1 was naïve and unaware of the experimental design, and S2 was one of the authors. Each subject had normal or corrected-to-normal vision, normal visual fields, and clinically normal eye movements. CFFs were measured using T.K.K.501c (Takei Scientific

Instruments Co. Ltd., Niigata, Japan) and estimated to be 38.1 and 36.0 Hz for S1 and S2, respectively. Informed consent, based on the Helsinki Declaration, was obtained from each subject. All experimental procedures were approved by the Kyoto University Graduate School and Faculty of Medicine Ethics Committee.

Visual display

The visual apparatus was similar to that used in our previous studies (Miura et al., 2009). The subjects faced a 19-inch CRT monitor (Eizo T766, positioned 63.4 cm in front of the eyes in a dark room. Visual stimuli were presented on the monitor (resolution, 1280 × 960 pixels; vertical refresh rate, 100 Hz). The subjects viewed the visual stimuli binocularly. RGB signals from the video card were converted to gray scale images with 11-bit resolution through an attenuator (Pelli and Zhang, 1991). A luminance look-up table with 256 luminance levels equally spaced from 0.0 to 10.0 cd/m^2 was created using direct luminance measurements (LS-100 photometer; Konica-Minolta, Japan) under software control. This table was then expanded to include 2048 equally spaced levels by interpolation.

Visual stimulus and procedures

We used the two-frame apparent motion of a vertical sinusoidal grating with a spatial frequency of 0.25 cycles/º, a Michelson contrast of 32%, and a mean luminance of 5.0 cd/m^2. We used this setting because the optimal spatial frequency for eye movement responses was about 0.25 cycles/º (Miura et al., 2009; Sheliga et al., 2005). We carried out two experiments using two-frame apparent motion of the sinusoidal grating patterns.

Experiment 1

At the beginning of each trial, a fixation target with a diameter of 0.5º appeared. The

subjects were instructed to look at the fixation target. After the right eye was positioned within ±2º from the fixation target for a randomized period between 500 and 1,000 ms, a sinusoidal grating appeared behind the fixation target. The initial phase of the sinusoidal grating was randomized from trial to trial at intervals of 1/8 of a wavelength. The subjects fixated on the target for a further 320 ms. The grating pattern was then replaced by a uniform gray image with a mean luminance the same as that of the former pattern (ISI). The ISI was set to 0, 10, 20, 30, 40, 60, 80, 160, 320 or 640 ms. The fixation target was then turned off and the second grating pattern, which was shifted from the initial grating by 1/4 of a wavelength rightward or leftward, appeared. The second frame was presented for 200 ms, after which the image was again replaced by a uniform gray with a mean luminance. This indicated the end of the trial. The next trial started one second after the end of the second frame. The subject was instructed only to fixate the fixation target when it was presented.

Experiment 2

At the beginning of each trial, a fixation target with a diameter of 0.5º appeared. After the right eye was positioned within ±2º of the fixation target for a randomized period between 500 and 1,000 ms, a sinusoidal grating appeared behind the fixation target. After a delay of 0, 10, 20, 30, 40, 60, 80, 160, 320, or 640 ms, the fixation target was turned off. Simultaneously, the second grating, which was shifted rightward or leftward from the initial grating by ¼ of a wavelength, appeared. We call this delay motion onset delay (MOD), as was done in the smooth pursuit experiments of Krauzlis and Lisberger (Krauzlis and Lisberger, 1994), who used this term to describe the interval between the appearance and the onset of motion of the small pursuit target. The second frame was presented for 200 ms, after which the image was replaced by a uniform gray with the same mean luminance, which indicated the end of the trial. The next trial started one second after the end of the second frame. The instruction to the subject was the

same as in experiment 1.

Data collection and analyses

All aspects of the experimental paradigm were controlled by two computers, as in previous studies (Miura et al., 2009; Miura et al., 2006). One computer ran the Real-time EXperimentation software package (REX) (Hays et al., 1982) for overall experimental protocol control; display, and data acquisition/storage. The other computer ran MATLAB (The Mathworks, MA) with the Psychophysics Toolbox extensions (Brainard, 1997) and generated the visual stimuli upon receiving a start signal from the REX machine.

Eye movements of the right eye were measured using a dual-Purkinje-image eye tracker system (Fourward Technology, VA, USA). Voltage signals encoding the horizontal and vertical components of the eye position were passed through an analog low-pass filter (-3 dB at 200 Hz) and digitized to a resolution of 12 bits, with sampling at 1 kHz. All data were stored and transferred to another PC for analysis using computer programs based on MATLAB. The eye-position data were smoothed using a 4-pole digital Butterworth filter (-3 dB at 25 Hz) and eye-velocity traces were derived from their two-point backward difference. Eye acceleration profiles were derived from the two-point backward difference of the eye-velocity traces and were used to detect saccades during the trials.

Our data analyses were restricted to ocular responses during the initial open loop periods. Changes in horizontal eye position were calculated during 80-ms periods beginning 80 ms after the onset of the second pattern, as the minimum latency of the ocular responses was ~80 ms. For the ISI or MOD stimulus condition, mean responses to leftward motion were subtracted from those to rightward motion to obtain response measures with better signal-to-noise ratios (S/N ratios). We also calculated 95% confidence intervals of the

differences to evaluate statistical significance. Based on our convention (rightward positive), ocular responses in the direction of the phase shift were positive, while those in the opposite direction were negative. The same procedure was applied to the mean eye velocity profiles for each stimulus condition to observe the time course of the ocular responses with better S/N ratios.

The motion energy model proposed by Adelson and Bergen (1985) was used to characterize the influence of ISIs and MODs. For simplicity, we used a single spatial channel model that consisted of even and odd Gabor filters with the center spatial frequency of 0.25 cycles/° and a spatial constant of 1.5°. These parameters were chosen based on previous findings (Miura et al., 2009; Sheliga et al., 2005). The temporal filters used in this study were expressed as:

$$y(t) = (kt)^N e^{-kt}\left(\frac{1}{N!} - b\frac{(kt)^2}{(N+2)!}\right), \quad (1)$$

where *k*, *b,* and *N* are the time constant, the strength of the negative lobe, and the order, respectively. The fast and slow temporal filters each had different *Ns* (N_f and N_s) and were involved in the model. X-T images (sampled at 0.2° and 0.01 s) were generated and used as the inputs for the model. The luminances of the sinusoidal gratings were expressed as numbers between -1 and 1, with frequencies of 0.25 cycles/°. The output of the model was the opponent energy as a function of time, which represented the difference between the leftward and rightward motion energies. The computation of the opponent energy exactly followed the model expression described in Figure 18 in Adelson and Bergen (1985), as performed by Challinor and Mather (2010). As we assumed that visual motion signals are transmitted along the visuomotor pathway with the delay of 80 ms, the opponent energy was summed over the 80-ms interval starting from the onset of the second grating and was compared with the ocular responses. The two filter parameters (*k* and *b*) and a scale factor (*c*) were optimized so that the differences

between the predicted and the actual responses were minimized with $N_f = 6$ and $N_s = 9$.

Results

Dependence on ISI

A quarter wavelength step of a sinusoidal grating presented with an ISI elicited OFRs in the opposite direction to that of the actual step of the visual stimulus. Figure 1A shows the mean eye velocity profiles of one subject (S1) for different ISIs. In the absence of an ISI, the OFRs occurred fairly weakly in the direction of the stimulus shift. Addition of an ISI of 10 ms or more inverted the OFRs. The amplitude of the inverted OFRs was maximal when the ISI was 30 or 40 ms. When the ISI increased further, the ocular responses decreased and were almost extinguished when the ISI was 160 ms.

The quantification of the responses in terms of changes in eye position over the open-loop responses confirms our impressions from the mean eye velocity profiles. As shown in Figure 1B, the inverted OFRs were significant when the ISIs were 10, 20, 30, 40, 60, and 80 ms. Subject S2 replicated these effects of ISIs, although the magnitude of the OFRs were smaller than S1 (Figure 1C), The ocular responses were significant only when the ISIs were 20, 30, and 40 ms. These ISI-associated changes in the OFRs are quite similar to those found in previous studies (Shaliga et al., 2006; Nohara et al., 2015).

Dependence on MOD

Figures 1B and 1C show that net OFRs were fairly small or almost zero when the pattern step was presented without an ISI (i.e., 0 ms in Figures 1B and 1C). A second experiment was carried out to investigate potential causes for this phenomenon. We found that OFRs to 2-frame apparent motion were critically dependent on delays in the presentation of

pattern step (MODs).

Figure 2A shows mean eye velocity profiles under different MODs. The deflections of the eye velocity profiles increased as the MOD increased up to 30 ms, and then decreased gradually as the MOD increased further. The deflections reached the minimal level and the eye velocity profiles of the ocular responses showed relatively complex waveforms (deflected negative and positive). Figure 2B shows integrated responses during the open-loop interval, i.e., changes in eye position during the 80-ms interval starting from 80 ms after the onset of motion. These plots confirmed our intuitive impressions of the eye velocity profiles. The net OFRs were all in the same direction as the stimulus shift and were significant over the MODs tested. The responses were maximal when the MOD was 30 ms. The maximal response at a MOD of 30 ms was significantly larger than that at MODs of 60 ms or longer. Note that at a MOD of 640 ms, the response is shown by a gray line with a gray shaded area showing 95% confidence intervals. Another subject showed the same dependence on MODs, though the responses were smaller compared with S1 (Figure 2C).

Estimating the temporal filters

The results from these two experiments can be explained in a unifying manner if we assume that the OFRs are dominated by energy-based motion computations involving temporal filters with biphasic impulse response functions. We tested the relevance of this idea using a computer simulation. In the computer simulations, changes in eye position during the initial open loop are assumed to be proportional to the opponent energy of the model. The three parameters, k, b, and c of equation (1) were optimized assuming $N_f = 6$ and $N_s = 9$. The opponent motion energy of the motion energy model successfully reproduced the effects of MODs and ISIs with appropriate k, b, and c values ($R^2 > 0.95$), as shown in Figures 3A and B,

which show comparisons between actual data and predicted data obtained from the best-fit motion energy models for our two subjects. Figure 3C shows the impulse response functions of the best-fit fast (black lines) and slow (gray lines) temporal filters of subject S1, which were "biphasic". The Fourier transform of these filters indicated a band-pass characteristic broadly tuned with similar center frequencies 7.40 Hz and 6.30 Hz for the fast and slow filters, respectively. The impulse response functions of the other subject (S2) showed similar biphasic waveforms and frequency characteristics (optimal at 7.95 Hz and 6.70 Hz for the fast and slow filters, respectively).

Discussion

Comparisons with previous oculomotor studies

Previous studies have demonstrated the presence of inverted OFRs to quarter wavelength steps of sinusoidal gratings presented with an ISI (Nohara et al., 2015; Sheliga et al., 2006). In this study, we successfully replicated previous findings regarding the dependence on ISIs. In our previous study (Nohara et al., 2015), we pointed to the fact that OFRs to two frame apparent motion were fairly small when the ISI was zero. This phenomenon was also seen in the present study. Here we found that this phenomenon reflects the influence of delays in the appearance of the pattern step, i.e., MOD. As shown in Figure 2, the amplitudes of the responses critically depended on MOD. Note that this is the first evidence indicating the influence of the exposure duration of the initial stationary image on OFRs. Our results suggest that longer exposure to the stationary image prior to visual motion reduces the driving signals of the OFR. This may also explain why OFRs are strongest when visual motion starts immediately after saccades. It has been known that OFRs are largest tens of milliseconds after the end of saccades and gradually decrease as the interval between the onset of stimulus motion and the end of

saccade increases. This phenomenon is referred to as “post-saccadic enhancement” (Kawano and Miles, 1986; Takemura and Kawano, 2006). The post-saccadic delay of the onset of stimulus motion regulates the time of exposure to stationary image patterns prior to the onset of visual motion. Thus, the effects of MODs may contribute to the post-saccadic enhancement of the OFRs.

Previous studies have demonstrated that the initiation of smooth pursuit eye movement is affected by delays in the appearance of target motion, i.e. MOD (Krauzlis and Lisberger, 1994; Miura et al., 2001; Tabata et al., 2006). However, the dependence of smooth pursuit on MODs was fairly different from that observed for OFRs here. The initial acceleration of smooth pursuit was continuously increased as the MOD increased by one second, and was then slightly decreased, but maintained at a higher level for longer MODs. On the other hand, the influence of MOD on the OFRs showed a more rapid process. This difference suggests that our present findings are due to different mechanisms from those underlying the previous observations.

The mechanism

The present results can be explained by the following unified framework: 1) the energy-based mechanisms of visual motion analyses underlie the OFRs, and 2) the temporal filters embedded in this mechanism have “biphasic” impulse responses. This framework has been introduced to interpret the effects of the ISI (Pantle and Turano, 1992; Shioiri and Cavanagh, 1990). In this framework, temporal filters with a biphasic impulse response function produce an afterimage with a reversed contrast with respect to the first grating pattern (the grating with 180° phase difference) during an ISI. The motion between this reversed image and the second frame results in motion in the opposite direction to the actual image shift. On the other hand, the effects of moderate MODs can be interpreted as a holding process of the initial

stationary patterns caused by the temporal filters. The “effective” contrast of the initial pattern changes due to the temporal filters, even if the image on the monitor is unchanged. The net motion energy generated by the initial and the second patterns critically depended on effective contrast of the initial pattern. This explanation may not be so intuitive, as observers usually perceived the initial pattern as it was even under the longest MODs, where OFRs were almost absent. This phenomenon may be explained by the fact that our visual system processes form information and motion separately. In sum, the characteristics of OFRs under different MODs and those under different ISIs may be explained by, respectively, the onset and offset dynamics of the responses of visual motion systems to the first image pattern.

The motion energy model reproduced the response characteristics obtained under different MODs and those under different ISIs after quantitatively adjusting the parameters of the temporal filters. These results support the ideas described in the previous paragraph. Furthermore, the best-fit energy model provides quantitative estimates of the temporal filters of the visual motion system. The values of b for the temporal filters are 0.94 and 0.92 for S1 and S2, respectively. These values result in large negative lobes for the filter kernels which induce strong adaptations to the initial pattern and strong reversals after the offset of the initial pattern. The parameter k determines the time scale, which can be used to infer temporal frequency characteristics. Fourier analyses of these temporal filters provided us with quantitative estimates of the frequency characteristics involving the optimal temporal frequency, the cut-off frequency, and so on. The two subjects showed that critical flicker frequencies of 38.1 and 36.0 Hz, which corresponded to temporal frequencies resulting in 3% or 2% of maximal power in the fast temporal filters of the individual subjects.

Comparisons with psychophysical studies

Previous studies have demonstrated that the perceived direction reverses when two-frame apparent motion is presented with ISIs in humans (Boulton and Baker, 1993; Braddick, 1980; Pantle and Turano, 1992; Shioiri and Cavanagh, 1990; Takeuchi and De Valois, 1997). Shioiri and Cavanagh (1990) and Pantle and Turano (1992) have explained the effects of the ISI by assuming that the motion detectors receive the signals mediated by the temporal filters with biphasic impulse responses. As described above, several researchers have studied the effects of ISIs on perceived direction by using the motion energy model (Strout et al., 1994; Takeuchi and De Valois, 1997). However, these studies did not provide quantitative estimates of the temporal filters.

Several previous studies have demonstrated that temporal impulse response functions underlie human psychophysical responses in different ways (Burr and Morrone, 1993; Hisakata and Murakami, 2008; Kelly, 1961b). Kelly (1961b) estimated impulse response functions based on data from contrast sensitivity to flickering images at different temporal frequencies and showed a biphasic impulse response function, which had an intercept at 20 ms and ceased by about 100 ms. Burr and Morrone (1993) and Hisakata and Murakami (2008) estimated impulse response functions, which had with biphasic temporal profiles with intercepts at <100 ms and ceased by 150-200 ms. These profiles were based on data obtained using double-pulse presentation methods. In the present study, we obtained biphasic impulse response functions similar to those estimated by Burr and Morrone (1993) and Hisakata and Murakami (2008). The contrast sensitivities observed at different temporal frequencies by Burr and Morrone (1993) are also similar to the frequency characteristics of the temporal filters estimated here.

Challinor and Mather (2010) applied the motion energy model to reproduce the percepts to two-stroke apparent motion and estimated impulse response functions with biphasic profiles. For their procedures, the estimated value of k of the fast temporal filters (a temporal

scale factor in the model) was about 110, and b = 0.9 under N_f= 6 and N_s = 9. These values are similar to those in our present data (see Figures 3A and B), suggesting similarity between the temporal filters underlying the motion percept observed by Challinor and Mather (2010) and those of our OFRs.

Limitations and benefits

In the present study, we quantitatively estimate the temporal filters of the visual systems based on OFRs. The limitation of this approach is that one can only know the properties of low-level visual processing, as OFRs are thought to be largely dominated by low-level energy-based mechanisms (Miura et al., 2006; Sheliga et al., 2005). On the other hand, perceived motion is affected not only by low-level, but also by high-level mechanisms of visual motion analyses (Burr and Thompson, 2011; Nishida, 2011; Nohara et al., 2015). Thus, the current approach with the OFR may be beneficial when one attempts to effectively isolate low-level visual processing mechanisms from high-level ones.

We found complex waveforms of the OFRs when the MOD was 320 ms or more in experiment 2. These temporal dynamics were not fully explained by the dynamics of the simplest form of the motion energy model that we used. One possible explanation is that this complexity might be due to characteristics of the visuomotor pathway along which the visual signal is transformed into the motor command. Currently we do not have methods/data to specify the mechanism. Therefore, this question is still open.

Both the MOD and ISI experiments may not be necessarily required to obtain quantitative estimates of the filters, and either MOD or ISI experiment might be sufficient to estimate the temporal filters because there is no unconstrained parameter even when either one is selected to use. Thus, in a practical use, we will have some options when we collect the data

to fit the model, i.e., a mixture of the MOD and ISI experiments or either MOD or ISI experiment. A mixture experiment may be more useful to confirm whether the estimated temporal filters can reproduce the entire behaviors from the onset to the offset of the visual stimulus.

The OFR is a part of the optokinetic responses that are purely reflexive. Thus, it is able to be objectively measured. One benefit of using reflexive eye movements is that the subjects are not required to answer anything about the stimulus. Therefore, this method may be used in ophthalmological testing of human subjects who cannot appropriately understand/answer experimenters' questions. Furthermore, this approach may be usable for animals that show OFRs or optokinetic responses for scientific purposes. Thus, the present method is applicable in characterizing the visual systems of a wide variety of subjects in clinical/scientific fields.

Acknowledgement:

This work was supported by JSPS.KAKENHI Grant Number 15K06709 and in part by Translational Research Network Program, Japan Agency for Medical Research and Development (AMED).

Figure legends

Figure 1: A: Eye velocity profiles of subject S1's ocular responses to two-frame apparent motion stimuli presented with an ISI. Upward deflections denote eye movements in the direction of the quarter wavelength step. The gray-shaded area indicates the 95% confidence intervals of the eye velocity profiles. The corresponding ISI is indicated at the top of each panel. B and C: Dependence on ISIs for S1 (B) and S2 (C). Changes in eye position during the 80-ms interval starting from 80 ms after onset of the second pattern frame are plotted as a function of the ISIs. Error bars are 95% confidence intervals. The response under the 640-ms ISI is indicated by horizontal gray line with a 95% confidence interval indicated by the gray-hatched region.

Figure 2: A: Subject S1's eye velocity profiles of ocular responses to two-frame apparent motion stimuli under various MODs. Upward deflections denote eye movements in the direction of the quarter wavelength step. The gray-shaded area indicates 95% confidence intervals of the eye velocity profiles. The corresponding ISI is indicated at the top of each panel. B and C: Dependence on MODs for S1 (B) and S2 (C). Changes in eye position during the 80-ms interval starting from 80 ms after onset of the second pattern frame are plotted as a function of the MODs. Error bars are 95% confidence intervals. The response under the 640-ms MOD is indicated by a horizontal gray line with a 95% confidence interval indicated by the gray-hatched region.

Figure 3: A: Estimations of the temporal filters. A and B: Outputs of the best-fit motion energy models for S1 (A) and S2 (B) (black filled circles). The actual data are also plotted for reference (open squares). The responses under MODs (0-320 ms) and ISIs of 10-320 ms are plotted as

functions of the time of onset of the second frame from the onset of the first image frame. C and D: Temporal filters involved in the best-fit motion energy models for S1 (C) and S2 (D). The fast and slow filters are plotted by black and gray lines, respectively. E and F: Estimated frequency characteristics of the temporal filters. The characteristics of the fast and slow filters are plotted by black and gray lines, respectively.

References

Adelson, E.H., Bergen, J.R., 1985. Spatiotemporal energy models for the perception of motion. Journal of the Optical Society of America A 2, 284-299.

Boulton, J.C., Baker, C.L., Jr., 1993. Dependence on stimulus onset asynchrony in apparent motion: evidence for two mechanisms. Vision Res 33, 2013-2019.

Braddick, O.J., 1980. Low-level and high-level processes in apparent motion. Philos Trans R Soc Lond B Biol Sci 290, 137-151.

Brainard, D.H., 1997. The Psychophysics Toolbox. Spatial Vision 10, 433-436.

Burr, D., Thompson, P., 2011. Motion psychophysics: 1985-2010. Vision Research 51, 1431-1456.

Burr, D.C., Morrone, M.C., 1993. Impulse-Response Functions for Chromatic and Achromatic Stimuli. Journal of the Optical Society of America a-Optics Image Science and Vision 10, 1706-1713.

Challinor, K.L., Mather, G., 2010. A motion-energy model predicts the direction discrimination and MAE duration of two-stroke apparent motion at high and low retinal illuminance. Vision Res 50, 1109-1116.

Gellman, R.S., Carl, J.R., Miles, F.A., 1990. Short latency ocular-following responses in man. Visual Neuroscience 5, 107-122.

Hays, A.V., Richmond, B.J., Optican, L.M., 1982. A UNIX-based multiple process system for real-time data acquisition and control. WESCON Conference Proceedings 2, 1-10.

Hisakata, R., Murakami, I., 2008. The effects of eccentricity and retinal illuminance on the illusory motion seen in a stationary luminance gradient. Vision Res 48, 1940-1948.

Kawano, K., Miles, F.A., 1986. Short-latency ocular following responses of monkey. II.

Dependence on a prior saccadic eye movement. Journal of Neurophysiology 56, 1355-1380.

Kelly, D.H., 1961a. Visual Responses to Time-Dependent Stimuli .1. Amplitude Sensitivity Measurements. Journal of the Optical Society of America 51, 422-&.

Kelly, D.H., 1961b. Visual Responses to Time-Dependent Stimuli .2. Single-Channel Model of Photopic Visual System. Journal of the Optical Society of America 51, 747-&.

Krauzlis, R.J., Lisberger, S.G., 1994. Temporal properties of visual motion signals for the initiation of smooth pursuit eye movements in monkeys. Journal of Neurophysiology 72, 150-162.

Miles, F.A., Kawano, K., Optican, L.M., 1986. Short-latency ocular following responses of monkey. I. Dependence on temporospatial properties of visual input. Journal of Neurophysiology 56, 1321-1354.

Miura, K., Kobayashi, Y., Kawano, K., 2009. Ocular responses to brief motion of textured backgrounds during smooth pursuit in humans. Journal of Neurophysiology 102, 1736-1747.

Miura, K., Matsuura, K., Taki, M., Tabata, H., Inaba, N., Kawano, K., Miles, F.A., 2006. The visual motion detectors underlying ocular following responses in monkeys. Vision Res 46, 869-878.

Miura, K., Suehiro, K., Yamamoto, M., Kodaka, Y., Kawano, K., 2001. Initiation of smooth pursuit in humans. Dependence on target saliency. Exp Brain Res 141, 242-249.

Nishida, S., 2011. Advancement of motion psychophysics: review 2001-2010. J Vis 11, 11.

Nohara, S., Kawano, K., Miura, K., 2015. Difference in perceptual and oculomotor responses revealed by apparent motion stimuli presented with an interstimulus interval. Journal of Neurophysiology 113, 3219-3228.

Pantle, A., Turano, K., 1992. Visual resolution of motion ambiguity with periodic luminance- and contrast-domain stimuli. Vision Research 32, 2093-2106.

Pelli, D.G., Zhang, L., 1991. Accurate control of contrast on microcomputer displays. Vision Research 31, 1337-1350.

Sheliga, B.M., Chen, K.J., FitzGibbon, E.J., Miles, F.A., 2005. Initial ocular following in humans: a response to first-order motion energy. Vision Res 45, 3307-3321.

Sheliga, B.M., Chen, K.J., FitzGibbon, E.J., Miles, F.A., 2006. The initial ocular following responses elicited by apparent-motion stimuli: Reversal by inter-stimulus intervals. Vision Res 46, 979-992.

Shioiri, S., Cavanagh, P., 1990. ISI produces reverse apparent motion. Vision Research 30, 757-768.

Strout, J.J., Pantle, A., Mills, S.L., 1994. An energy model of interframe interval effects in single-step apparent motion. Vision Res 34, 3223-3240.

Tabata, H., Miura, K., Taki, M., Matsuura, K., Kawano, K., 2006. Preparatory gain modulation of visuomotor transmission for smooth pursuit eye movements in monkeys. Journal of Neurophysiology 96, 3051-3063.

Takemura, A., Kawano, K., 2006. Neuronal responses in MST reflect the post-saccadic enhancement of short-latency ocular following responses. Exp Brain Res 173, 174-179.

Takeuchi, T., De Valois, K.K., 1997. Motion-reversal reveals two motion mechanisms functioning in scotopic vision. Vision Research 37, 745-755.

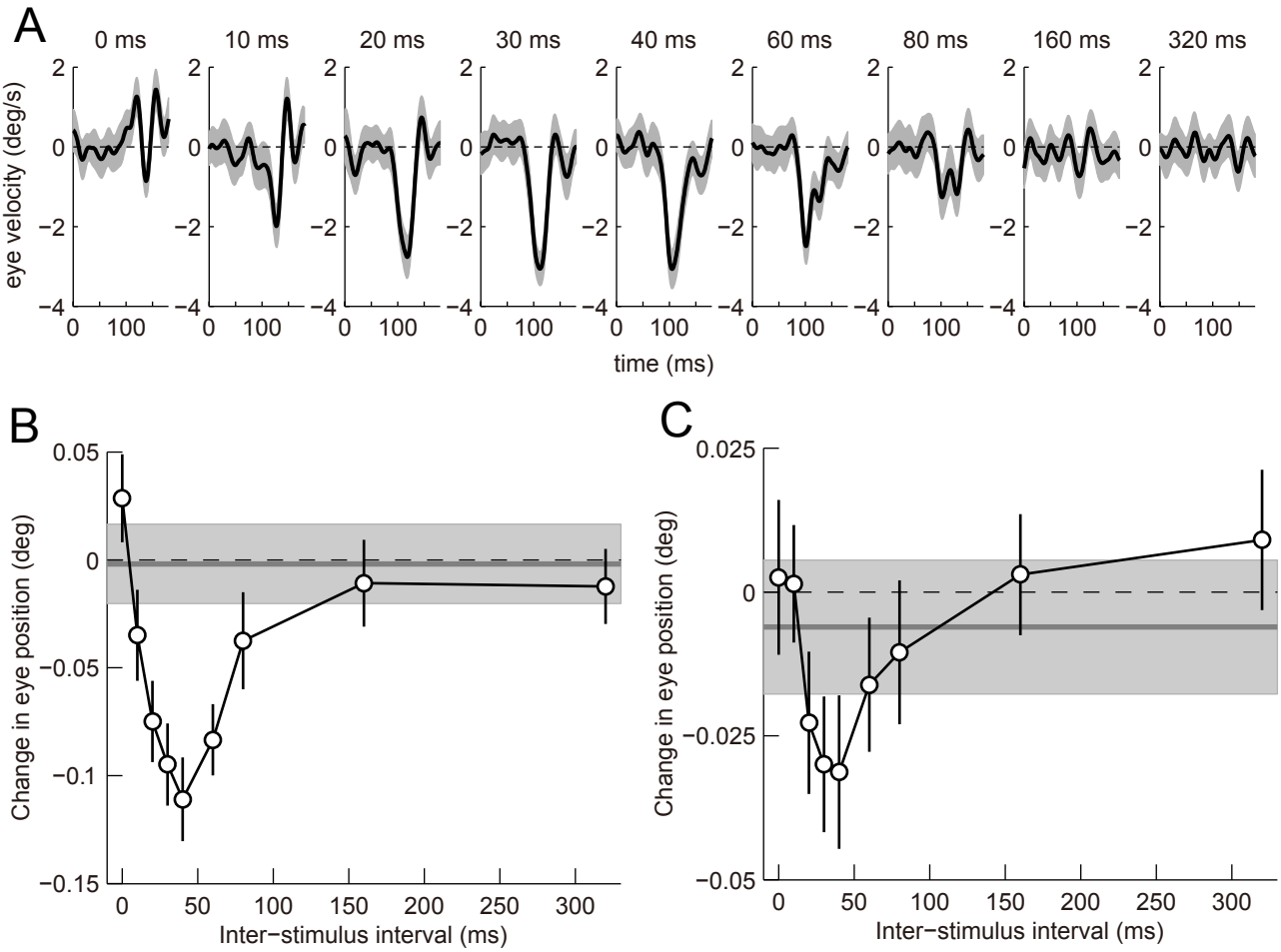
A
0 ms
10 ms
20 ms
30 ms
40 ms
60 ms
80 ms
160 ms
320 ms
eye velocity (deg/s)
time (ms)
B
Change in eye position (deg)
Inter−stimulus interval (ms)
C
Change in eye position (deg)
Inter−stimulus interval (ms)

Figure 1

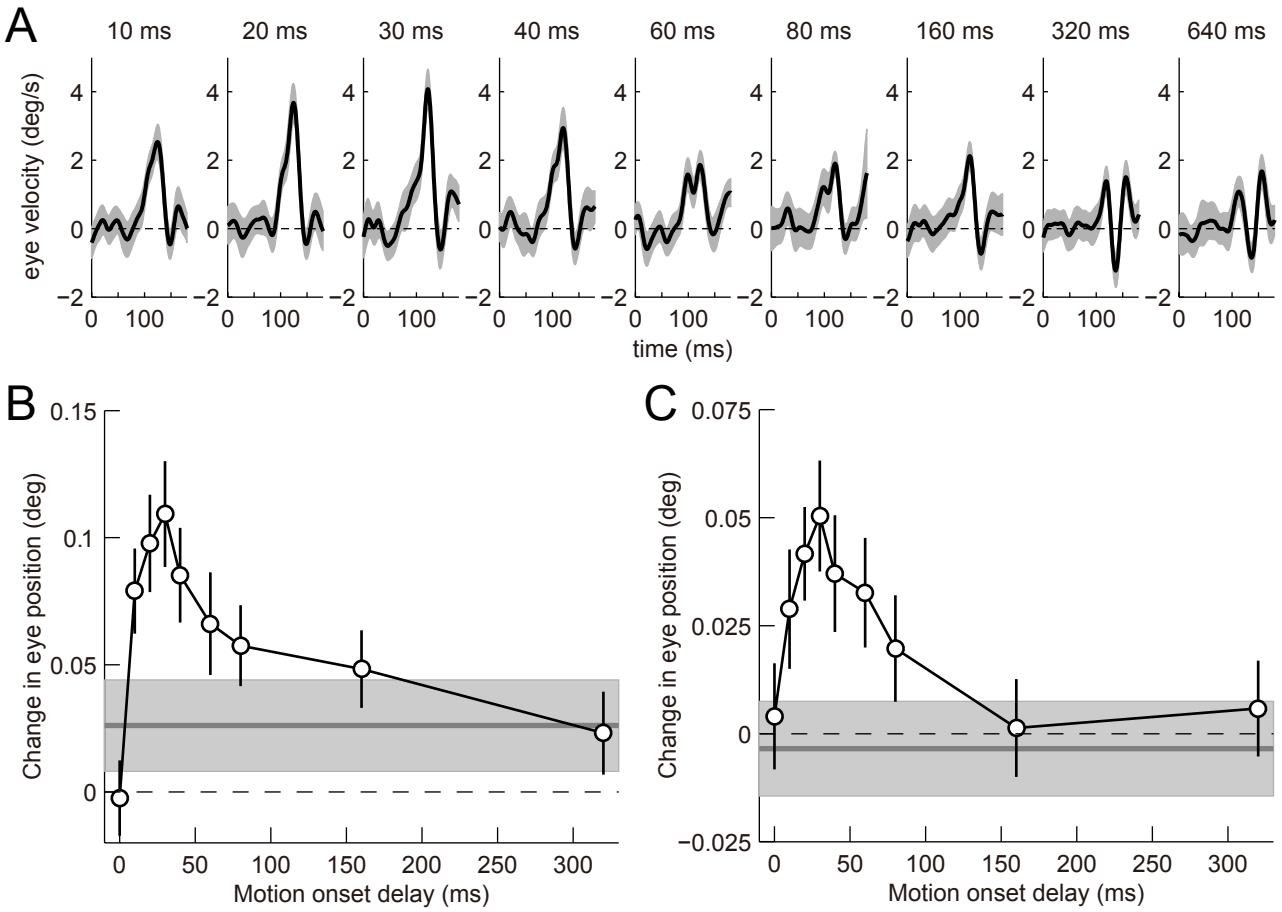
A
10 ms
20 ms
30 ms
40 ms
60 ms
80 ms
160 ms
320 ms
640 ms
eye velocity (deg/s)
time (ms)
B
Change in eye position (deg)
Motion onset delay (ms)
C
Change in eye position (deg)
Motion onset delay (ms)

Figure 2

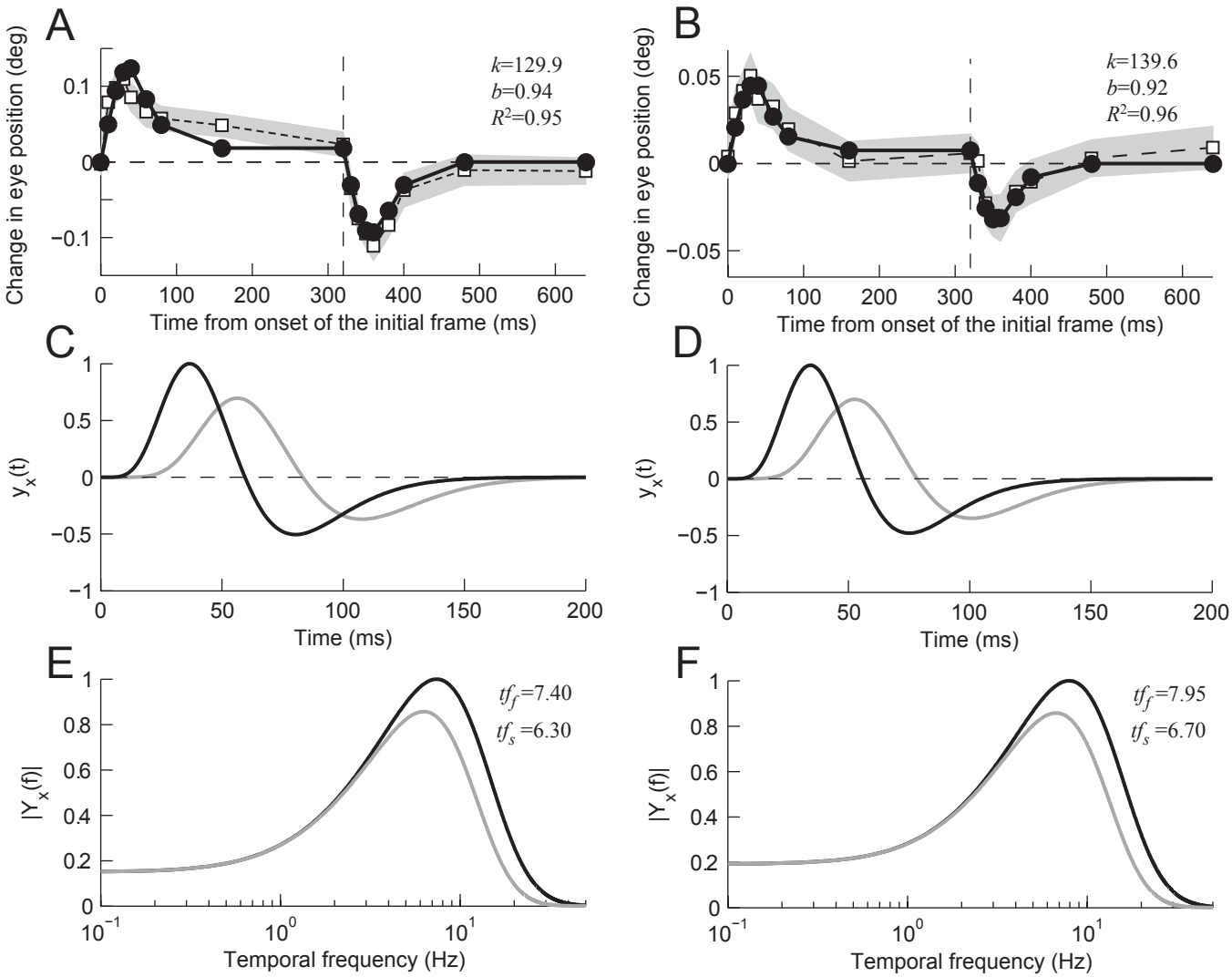
A
B
C
D
E
F
Change in eye position (deg)
Time from onset of the initial frame (ms)
k=129.9
b=0.94
R²=0.95
k=139.6
b=0.92
R²=0.96
y_x(t)
Time (ms)
|Y_x(f)|
tf_f=7.40
tf_s=6.30
tf_f=7.95
tf_s=6.70
Temporal frequency (Hz)

Figure 3